U.S. Department of Commerce
National Oceanic and Atmospheric Administration
National Weather Service
National Centers for Environmental Prediction
5200 Auth Road
Camp Springs, MD 20746-4304

**Office Note 436**

# A FAMILY OF TERRAIN-FOLLOWING THETA-SIGMA HYBRID VERTICAL COORDINATES

R. James Purser*
Science Applications International Corp., Beltsville, Maryland

Mark Iredell†
Environmental Modeling Center, NCEP, Camp Springs, MD

January 2002



* email: jim.purser@noaa.gov
† email: mark.iredell@noaa.gov

**Abstract**

We investigate an algebraically simple family of hybrid vertical coordinates which possess the advantages of isentropic coordinates at high elevations but gradually and smoothly make the transition to terrain-following coordinates at the lower levels. The family of coordinates has parameters by which we can choose the approximate elevation characteristic of the broad transition between isentropic and terrain-following behavior, or the degree of 'dilution' of the coordinates at upper levels with 'sigma'. We illustrate the effects of these parameters on the vertical distribution of hybrid coordinate levels and we estimate the relative magnitudes of numerical truncation error associated with the calculation of the horizontal pressure gradient force as the result of using either pressure and geopotential or Montgomery potential and potential temperature as dependent variables. We claim no special merits for the particular family of hybrid coordinates we have employed here; rather we have used a relatively simple parameterized family as representative of a much larger class of hybrids, in the hope that the qualitative conclusions drawn from this study have a validity that extends more generally.

## 1. Introduction

For pressure, $p$, the standard 'sigma' vertical coordinate of Phillips (1957), defined:

$$\sigma = \frac{p}{p_*}, \tag{1.1}$$

or its convenient generalization to the case of a model with a top at finite pressure, $p_T$:

$$\sigma = \frac{p - p_T}{p_* - p_T}, \tag{1.2}$$

where $p_*$ denotes the terrain-level pressure, have the valuable property that the terrain surface itself coincides with a constant value of the vertical coordinate, but share the unfortunate defect of imposing a strong imprint of the topographic profile upon the elevation of the coordinate surfaces at all levels below the top. As a result, the calculation of each horizontal pressure gradient force component at any point in a grid column over steep terrain involves the extraction of a relatively small residual quantity from the difference of two large opposing terms. Percentage errors in the calculation of either of these terms usually leads to a greatly amplified percentage error in the desired residual. Errors of this kind can have various manifestations, depending on details of the formulation of the model, and, in the worst cases, can lead directly to significant persistent errors in the forecasts. There are remedies that work well with certain special forms of the vertical thermal profile (e.g., Corby et al. 1972) but there seems to be no scheme seems entirely satisfactory with all possible profiles. For a discussion of these problems, see Mesinger and Janjić (1985) and Janjić (1989).

Within the context of terrain-following coordinates, there is apparently no completely satisfactory remedy to the aforementioned problem of estimating an accurate horizontal pressure gradient. However, by judicious modifications to the definition of the vertical coordinate, it is

at least possible to confine the vertical extent of this problem to a relatively small fraction of the vertical column close to the ground. At higher altitudes, we may choose to let the coordinates tend either towards a quasi-horizontal family of surfaces, such as contant-$p$ or constant-$z$ (geometrical height above mean sea level) or towards the family of isentropic surfaces defined by the condition that potential temperature $\theta$ is constant on each surface. In these special cases, for a hydrostatic model, the horizontal pressure gradient force *is* expressible as some multiple of the gradient on the coordinate surface of a *single* potential. However, the isentropic family of vertical coordinates is especially attractive for other reasons. For one, the atmospheric motion is largely confined to be a flow approximately tangent to these surfaces (the exception occurs only where diabatic forcings are strong). Therefore, where the vertical coordinate becomes close to isentropic, the truncation errors associated with vertical advection tend to be substantially reduced because, in effect, there is very little 'vertical' advection going on, relative to the coordinate system adopted. Eliassen and Raustein (1968, 1970) were early pioneers in the application of purely isentropic vertical coordinates in atmospheric models. Various forms of the governing equations in generalized vertical coordinates were provided by Kasahara (1974). More recent developments (Bleck 1978, Uccellini et al. 1979, Zhu et al. 1992, Bleck and Benjamin 1993, Konor and Arakawa 1997) recognize the value of 'hybridizing' the $\theta$ variable with $\sigma$ at low levels in order to keep the convenience of terrain following coordinates. The beneficial consequences of a hybrid coordinate system for the treatment of the long-range transport of water vapor in a general circulation model have been documented by Johnson et al. (1993), although their coordinate system involves a sharp interface separating theta levels above from sigma levels below. Another reason to favor an approximately isentropic coordinate is that, within vertical zones of pronounced thermal inversion, where the horizontal velocity and humidity variables tend to change rapidly, the isentropic coordinates automatically enhance the resolution of these zones. One might therefore reasonably hope that, through the adoption of an approximately isentropic vertical coordinate, the overall *effective* vertical resolution of the model becomes correspondingly enhanced.

While admitting the potential advantages we have just mentioned, we should temper our enthusiasm for the isentropic 'theta-hybrid' coordinates with the recognition that difficulties can arise, not only from the intrusion of elevated or warm terrain, but, even at high altitudes, from the multi-valuedness of $\theta$ with height that can occur in association with vertically well-mixed layers. To allow for such occurrences, the formulation of any hybrid coordinate system must be provided with appropriate safeguards to ensure that, even in the midst of a well mixed layer, the coordinate increases smoothly and monotonically with height.

In this note we explore the behavior of a family of hybrid theta-sigma coordinates which smoothly makes the transition from a sigma-like terrain-following system near the ground towards an isentropic coordinate system aloft, but which never attains the status of a *pure* isentropic coordinate system within the model's interior. By always mixing a positive amount of 'sigma' in the coordinate definition, we avoid the difficulties associated with mixed layers, even at higher altitudes (where mixing can still occur as a result of breaking gravity waves and other processes). Our proposed family of coordinates is also given sufficient generality to include the cases of the pure sigma-like coordinate systems for which the top level is one of constant pressure; these special cases occur at the extreme value of one of the parameters of the family. Since these sigma-like coordinates are already in use in existing models, the generalization of the

vertical coordinate proposed here should facilitate the testing and development of the auxiliary components of these models, such as, for example, the semi-implicit solvers, in a progressive migration towards the goal of a theta-hybrid vertical coordinate framework. For example, the techniques that are successful in making a sigma coordinate model semi-implicit often rely on a vertical spectral decomposition which may not be immediately applicable in the intended theta-hybrid coordinate. However, by examining the numerical behavior of a model using a vertical coordinate with some intermediate formulation, as is permitted by the general family of coordinates we propose, it may be relatively simple to determine the appropriate remedial modifications that the hybrid coordinate requires.

The next section describes the algebraic construction of simple hybrid coordinates possessing desirable properties. Section 3 investigates the horizontal pressure gradient errors associated with different coordinates under the idealized assumption of negligible vertical discretization errors, and Section 4 concludes.

## 2. Constructing hybrid coordinates

It is convenient to adhere to the convention that all our putative hybrid coordinates are 'rectified', or oriented so as to increase with increasing altitude, and go from zero at the ground to one at the model top. The families of hybrid coordinates are composed of suitable mixtures of potential temperature (which usually increases with height) and either hydrostatic pressure (which decreases with height) or geopotential height itself. To simplify the construction and interpretation of the hybrids, it is also convenient to rectify and normalize the scales of potential temperature and pressure such that their normalized versions tend mainly to increase with height with a value of unity representing either the model top or at least some comparable altitude, and such that the terrain value of the normalized quantity is some positive value closer to zero than to unity. For example, we define the rectified and nondimensionalized pressure-type variable,

$$\hat{p} = \frac{p_L - p}{p_L - p_T}, \tag{2.1}$$

and rectified sigma-type variable,

$$\hat{\sigma} = \frac{\hat{p} - \hat{p}_*}{1 - \hat{p}_*}, \tag{2.2}$$

for some constant standard reference pressure, $p_L$, somewhat larger than any typical pressure at the ground or at sea-level. Another standard pressure, $p_0$, (typically chosen to be 1000 mb) is used in the definition of the potential temperature:

$$\theta = T \left( \frac{p_0}{p} \right)^{\kappa}, \tag{2.3}$$

with Poisson's constant $\kappa$ defined in terms of the gas constant $R$ and the constant-pressure specific heat, $C_p$:

$$\kappa = \frac{R}{C_p} = 2/7. \tag{2.4}$$

The rescaling of potential temperature will involve setting one constant value, $\theta_T$, characterizing the model top, and another constant value, $\theta_L$, required to be slightly smaller that any actual

value of $\theta$ encountered within the model domain. The rescaled potential temperature, $\hat{\theta}$, is then defined:

$$\hat{\theta} = \frac{\theta - \theta_L}{\theta_T - \theta_L}. \tag{2.5}$$

*(a) A hybrid p-σ coordinate*

For a positive constant, $\tau$, the term,

$$W = \frac{\tau}{\hat{\sigma}}(1 - \hat{p}), \tag{2.6}$$

has the properties: $W \gg 1$ when $\hat{\sigma} \ll 1$ and $W \to 0$ as $\hat{p} \to 1$. Therefore, the function,

$$\zeta = \frac{\hat{\sigma}\hat{p}}{\hat{\sigma} + \tau(1 - \hat{p})}, \tag{2.7}$$

acts as a hybrid coordinate that exhibits sigma-like terrain-following behavior where $\hat{\sigma} \ll 1$ but is more pressure-like as $\hat{p}$ becomes close to unity. Other pressure-sigma hybrid coordinates are described in Simmons and Burridge (1981) and Simmons and Strüfing (1981) in the context of the ECMWF's semi-implicit spectral model. Our 'transition parameter', $\tau$, exerts a degree of control over the proportions of the model atmosphere partitioned predominantly into terrain-following and pressure-like behavior for the coordinate $\zeta$. Fig. 1 illustrates the effect of the transition parameter by showing the elevations of vertical coordinate surfaces over a terrain surface whose elevation changes between zero and 4 km when the atmosphere is horizontally stratified. The coordinate values are increasing from 0 to 1 in 40 uniform increments of 0.025 in each case. Fig. 1a shows the rectified sigma coordinate, $\hat{\sigma}$. In comparison, the pressure-sigma hybrid coordinates given by (2.7) are shown in Fig. 1b for $\tau = 0.2$ and in Fig. 1c for $\tau = 0.5$. Both choices keep the upper coordinate surfaces more nearly horizontal than the corresponding sigma coordinate but, for the smaller value of $\tau$ the transition towards level coordinate surfaces tends to occur lower. For these examples the pressure constants are defined:

$$p_L = 1200 \text{ mb}, \tag{2.8}$$

$$p_T = 150 \text{ mb}. \tag{2.9}$$

*(b) A hybrid θ-σ coordinate*

The behavior of the weight function,

$$W = \frac{\tau}{\hat{\sigma}}(1 - \hat{\theta}), \tag{2.10}$$

is completely analogous to that of (2.6), but now, $W \to 0$ as $\hat{\theta} \to 1$. This immediately suggests the $\theta$-$\sigma$ hybrid coordinate analogous to (2.7):

$$\zeta = \frac{\hat{\sigma}\hat{\theta}}{\hat{\sigma} + \tau(1 - \hat{\theta})}. \tag{2.11}$$

However, the transition that parameter $\tau$ controls is now between $\sigma$-like behavior low down and more nearly isentropic behavior at upper levels. This function-based formulation of hybrid coordinates is somewhat closer conceptually to those of Zhu et al. (1992) or the even more general formulations discussed by Konor and Arakawa (1997) than the construction procedure described by Bleck and Benjamin (1993).

Fig. 2a shows the thermal profile (both temperature and potential temperature are plotted) for the stratification used to graph the coordinates of Fig. 1. For the same horizontally uniform stratification, Figs. 2b and 2c show the uniformly spaced $\zeta$ coordinates implied by (2.11) for $p_T = 150$ mb as before, and for the additional parameter choices:

$$\tau = 0.2, \tag{2.12}$$

$$\theta_L = 220 \text{ K}, \tag{2.13}$$

$$\theta_T = 390 \text{ K}. \tag{2.14}$$

In Fig. 2b and Fig. 2c we illustrate the effects of the transition parameter, $\tau$, whose values are respectively $\tau = 0.2$ and $\tau = 0.5$. In the former case, we see significant bunching of the coordinates near the ground over the higher reaches of the terrain but a relatively speedy transition towards predominantly $\theta$ coordinates above the upper inversion. In Fig. 2c there is much less intense bunching at the high ground and more gradual and prolonged transition towards $\theta$. This trend continues with still higher values of $\tau$, as we see in Fig. 3, which follows the format of Fig. 2 except with panels (b) and (c) corresponding to the parameter choices $\tau = 1.0$ and $\tau = 2.0$ respectively. In these cases, the enhancement of resolution within the lower inversion is very slight, becoming almost imperceptible near its intersection with the terrain. The resolution of the upper inversion remains high, owing to the fact that, at these higher altitudes, the hybrid coordinate remains dominated by the $\theta$ contribution and is only weakly influenced by the effect of terrain.

We note that the distributions of the coordinate surfaces shown in Figs. 2 and 3 are almost certainly not suitable choices for an actual model, where we would probably prefer to provide relatively higher vertical resolution in the boundary layer and give much less emphasis to resolving the stratosphere. These illustrations merely show the level distributions for *equally*-spaced values of the coordinate $\zeta$; there is, of course, nothing to prevent levels of an actual model from being chosen from a *non*-uniform distribution in $\zeta$ if desired, provided such a distribution is at least derived from a smoothly varying function of $\zeta$ so as not to degrade the quality of vertical numerical differencing and other standard discrete operators that a model requires.

### (*c*) *Generalization to include sigma coordinates as a special case*

For model development it is useful to formulate the hybrid coordinates within a family sufficiently general to include the sigma coordinates as a special case. If the parameterization of the family is continuous, this then allows model code originally designed to run in sigma coordinates to be adapted, without loss of continuity, to the more general coordinates that incorporate the theta-sigma hybridization. One way to proceed is to define a new variable $v$ to be a simple mixture of $\hat{\theta}$ and $\hat{p} - \hat{p}_*$, where $\hat{p}_*$ is the value of $\hat{p}$ at the ground, and $\hat{p}$ is as defined in (2.1). We let $\alpha$ be the mixing parameter:

$$v = (1 - \alpha)\hat{\theta} + \alpha(\hat{p} - \hat{p}_*), \tag{2.15}$$

and define the value this quantity is to have at the model top by:

$$v_T = 1 - \alpha \hat{p}_*. \tag{2.16}$$

Our generalization of the hybrid coordinate,

$$\zeta = \frac{\hat{\sigma}\frac{v}{v_T}}{\hat{\sigma} + (1-\alpha)\tau(v_T - v)}, \tag{2.17}$$

is then easily shown to give the expression (2.11) when $\alpha = 0$ and to give $\zeta = \hat{\sigma}$ when $\alpha = 1$. For intermediate values of $\alpha$, we obtain a coordinate system possessing some features of the theta-sigma hybrid. For example, Fig. 4 shows the new generalized coordinate, for the same horizontally uniform thermal profile (Fig. 4a), with $\tau = 0.5$ and with other coordinate parameters the same, but now using (2.17) with (b) $\alpha = 0.2$ and (c) $\alpha = 0.8$. Compared with the corresponding $\alpha = 0$ case, which is identical to Fig. 2c, the effect of the small positive $\alpha$ is seen in Fig. 4b to show up as a slightly reduced resolution of the lower inversion and the slight additional tilting of all the coordinate surfaces, especially those at upper levels where, formerly, the terrain had very little influence. For the much larger value of $\alpha = 0.8$ shown in panel (c) the terrain seems to be the dominating influence and the enhancement of resolution within the inversions is almost negligible. Of course, for the further augmented choice, $\alpha = 1$, we would obtain the 'generalized sigma' distribution of Fig. 1a once more.

(*d*) *Remarks*

In the construction of these hybrid coordinates we have used a definition of $\hat{\sigma}$ based on pressure. In a nonhydrostatic model, it would probably be more appropriate to employ the 'hydrostatic pressure' here, based on vertical mass-integals, which would allow a natural generalization of the form of dynamics advocated by Laprise (1992). Alternatively, there is an equally valid family of hybrid coordinates corresponding to each of the families, (2.7), (2.11) and (2.17), in which we replace the rectified pressure (including in the definition of $\hat{\sigma}$) by a normalized geopotential, defined by analogy to (2.1):

$$\hat{\phi} = \frac{\phi_L - \phi}{\phi_L - \phi_T}, \tag{2.18}$$

so that the corresponding definition of $\hat{\sigma}$ in (2.2) is now equivalent to the height-based terrain-following coordinate proposed by Gal-Chen and Somerville (1975). Other variations on the same algebraic theme are obtained for the theta-hybrid coordinate by, for example, replacing $\theta$ by the (dry) entropy, or any other smooth and monotonic function of $\theta$.

## 3. Horizontal pressure gradient errors

In the vicinity of steep terrain, all terrain following coordinate systems engender errors in the computation of the horizontal pressure gradient force. This occurs even when the actual atmosphere is perfectly stratified into horizontal layers so that there is no actual pressure

gradient component in the horizontal. If we employ pressure $p$ and geopotential $\phi$ as the dependent variables for these calculations, with the density given by $\rho$, we must use the identity:

$$\frac{1}{\rho}\nabla_\phi p = \frac{1}{\rho}\nabla_\zeta p + \nabla_\zeta \phi, \tag{3.1}$$

which holds in both hydrostatic and, with minor modification to the last term, to nonhydrostatic circumstances. Fig. 5 reproduces the same thermal profile as before (a) together with a contouring of the spurious pressure gradient obtained with the generalized sigma coordinates, $\hat{\sigma}$ defined by (2.2) when the horizontal width of the sloping terrain is 600 km, resolved with 40 grid intervals of 15 km, and when centered second-order (b) and fourth-order (c) spatial differencing is used to estimate the derivatives of $\phi$ and $p$ along the $\hat{\sigma}$ surface. In these idealized calculations, we only include the contributions to the truncation errors arising from the quasi-horizontal differencing, implicitly assuming these errors to be dominant in practice, which would be essentially the case for a dense vertical distribution of model levels. (In experiments not shown here, the errors are reduced when the horizontal grid resolution is enhanced.) Contours are at intervals of $10^{-5}$ m s$^{-2}$ or, in terms of an equivalent geostrophic wind magnitude, about 0.1 m s$^{-1}$ for a Coriolis parameter of $10^{-4}$ s$^{-1}$. Contours are staggered with respect to zero, in order to minimize the visual noise. Clearly, without changing the vertical coordinates, the numerical errors are significantly reduced merely by replacing the second-order differencing by fourth-order evaluations.

The effect of changing the vertical coordinate to the hybrid defined by (2.11) is seen in Fig. 6. The differencing is as in Fig. 5 and most of the coordinate parameters are as before and with $\tau = 0.5$. Already, we see a significant reduction in the errors, amounting essentially to the elimination of obvious error at the upper inversion. What errors remaining tend to be concentrated just above and below the lower inversion, rather than within the inversion layer itself, where the coordinate slope is smaller (see Fig. 2c). At fourth-order, the errors seem to be almost completely removed even at the lower inversion. However, we must bear in mind that the idealized thermal distribution, being horizontally uniform, is especially favorable to $\theta$-like coordinates to the extent that there is no horizontal thermal gradient present to tilt such coordinates. We shall see below that the calculations involving derivatives of pressure and geopotential are not free of significant errors for hybrid coordinates in a baroclinic environment; in such a case, the derivation of the horizontal pressure gradient force from derivatives of Montgomery potential, $M$, and potential temperature, $\theta$, might be more appropriate.

The Montgomery potential is defined in terms of conventional variables,

$$M = \phi + C_p T, \tag{3.2}$$

(Haltiner and Williams 1980) and, in a hydrostatic atmosphere, satisfies

$$\frac{\partial M}{\partial \theta} = \Pi, \tag{3.3}$$

where the Exner pressure function,

$$\Pi = C_p \left(p/p_0\right)^\kappa \tag{3.4}$$

multiplies the potential temperature, $\theta$, to give $C_pT$. The horizontal pressure gradient in a hydrostatic atmosphere is expressible,

$$\frac{1}{\rho}\nabla_\phi p = \nabla_\zeta M - \Pi\nabla_\zeta\theta. \tag{3.5}$$

Although one would certainly not use this combination of terms in a $\sigma$-coordinate model, it is nevertheless useful, for a comprehensive comparison, to see the extent of the cancellation of errors that occurs in this case with the same horizontally uniform profile. As we see in Fig. 7, where panels (b) and (c) again depict the errors that correspond to using second- and fourth-order differencing, these errors are now very large, exceeding the equivalent of 1 m s$^{-1}$ in implied geostrophic wind within the lower inversion at second-order and being almost as large in the fourth-order case. However, with the hybrid coordinates, $\tau = 0.5$, Fig. 8 shows that the errors within the upper inversion (where, being close to having $\theta$ coordinates, the Montgomery potential term almost completely dominates the pressure gradient calculation) are effectively eliminated, while the errors in the lower inversion are much reduced except at the terrain surface itself.

We have already remarked that using a horizontally stratified atmosphere for these error evaluations artificially favors the hybrid coordinates at upper levels. Therefore, we now consider the case in which the vertical profile in the center of the domain remains as it was before, but a horizontal thermal gradient is imposed, being a uniform 0.25 K per horizontal grid space on surfaces of constant pressure, and where the terrain variations are removed and surface pressure is constant. The geopotential for this solution is numerically integrated on a set of finely-spaced pressure levels, on which the 'true' pressure gradient (which now does *not* vanish) is calculated on these levels using eighth-order horizontal derivatives of the geopotential. Other mass variables (including the hybrid coordinate variable) are also computed on this vertically fine grid. Fig. 9 shows the coordinate surfaces that result from (2.17) with the same parameters as before except $\tau = 0.5$ and with, (b) $\alpha = 0$ (i.e., the coordinate belongs to the special family, (2.11)) and, (c) $\alpha = 0.2$, which 'dilutes' the theta-hybrid with additional 'sigma' at all levels. Visually, the differences between these two coordinate distributions are hard to see, being mainly a subtle reduction in the slope of the coordinates in the case of panel (c). For the coordinates of Fig. 9b, the errors arising from using the derivatives of pressure and geopotential at second- and fourth-order are shown respectively in Figs. 10b and 10c. As always, the use of higher-order differencing leads to a marked reduction in the magnitudes of the errors, which now tend to be localized to just above and below the upper inversion and just below the tropopause, where weakly stable stratification and strong baroclinicity combine. In terms of the equivalent geostrophic wind, the errors remain well below the 1 m s$^{-1}$ level and, since the geostrophic wind itself is almost two orders of magnitude greater than this at these levels, the percentage error we incur is probably acceptable. However, if we were to use Montgomery potential and potential temperature gradients instead, the errors (not shown) are quite negligible at these elevations, despite the steep coordinate slopes. Another way to reduce the errors for this atmospheric state without switching to the use of the Montgomery and potential temperature variables is to adopt the more general coordinate (2.17) with a small positive $\alpha$. Taking the case of the coordinate of Fig. 9c ($\alpha = 0.2$) leads to the errors shown in Fig. 11, which are substantially smaller than those of Fig. 10 in this particular atmosphere, especially in the case of fourth-order differencing.

## 4. Discussion and conclusions

In a series of relatively simple idealized atmospheric states, and with some equally idealistic assumptions that vertical discretization errors are relatively insignificant, we have investigated how the choice of vertical coordinate is likely to affect the size of the error in the calculation of the horizontal pressure gradient force in the presence of sloping terrain or in a baroclinic environment. We find in virtually every case that the errors implied by using fourth-order horizontal differences are much smaller than those resulting from using second-order differences. The trend continues at even higher orders, although we have not presented the results here. We also find that the problems that theta-hybrid coordinates have in elevated mixed or weakly stable layers, when the horizontal pressure gradient is computed as the difference between terms involving derivatives of pressure and geopotential from (3.1), are greatly alleviated when the coordinate definition includes a slight dilution with 'sigma', as occurs when the formula (2.17) is used with a small positive $\alpha$. Then, the errors at fourth-order seem well within acceptable bounds, even when using pressure and geopotential variables in the calculation. For a nonhydrostatic model, this is attractive because the force term is *completely* determined from just these two variables. The alternative use of the variables, Montgomery potential and potential temperature, leads to substantial further improvements in accuracy for the hydrostatic calculation of horizontal pressure gradient in even the simpler ($\alpha = 0$) theta-hybrid coordinates, but, in a nonhydrostatic model, the gradient of a third variable must be included to account for the full nonhydrostatic effect. For example, the addition to the right-hand side of (3.5) of a term proportional to the gradient of the geopotential, weighted by the nonhydrostatic residual vertical acceleration, is sufficient to correct this equation in the nonhydrostatic case (Zuwen He, personal communication).

On the basis of the results obtained here, we would certainly recommend using the Montgomery potential form, (3.5) of pressure gradient in any hydrostatic model that employs a theta-hybrid coordinate. With the modification mentioned above, this would probably be the best choice also for a nonhydrostatic model, although, provided high-order numerics are employed, the errors would still be acceptable even if the conventional pressure and geopotential variables were employed using (3.1), and then an additional calculation of a gradient would be avoided. However, for results of the best quality, regardless of whether we have a hydrostatic or nonhydrostatic model, we would recommend the combination of high-order spatial numerics, a theta-hybrid vertical coordinate (possibly with weak dilution with 'sigma' at all levels to avoid problems with mixed or weakly stratified layers at high altitudes), and the adoption of the Montgomery potential in the horizontal pressure gradient calculations to ensure that these force terms remain accurate over the largest extent of the domain under the widest range of typical conditions.

## Acknowledgment

We are grateful to Mr. Zuwen He for sharing with us his formulation of the nonhydrostatic dynamics of a model employing a general vertical coordinate. Discussions with Drs. Sajal Kar and Zavisa Janjić, who both reviewed the manuscript, and with Dr. Fedor Mesinger helped to clarify this study. This work was partially supported by the NSF/NOAA Joint Grants Program of the US Weather Research Program. This research is also in response to requirements and

funding by the Federal Aviation Administration (FAA). The views expressed are those of the authors and do not necessarily represent the official policy or position of the FAA.

## References


Bleck, R. 1978 On the use of hybrid vertical coordinates in numerical weather prediction models. *Mon. Wea. Rev.*, **106,** 1233–1244.

Bleck, R., and S. Benjamin 1993 Regional weather prediction with a model combining terrain-following and isentropic coordinates. Part I. *Mon. Wea, Rev.*, **121,** 1770–1785.

Corby, G. A., A. Gilchrist, and R. L. Newson 1972 A general circulation model of the atmosphere suitable for long period integrations. *Quart. J. Roy. Meteor. Soc.*, **98,** 809–832.

Eliassen, A., and E. Raustein 1968 A numerical integration experiment with a model atmosphere based on isentropic coordinates. *Meteor. Ann.*, **5,** 45–63.

Eliassen, A., and E. Raustein 1970 A numerical integration experiment with a six-level atmospheric model with isentropic information surface. *Meteor. Ann.*, **5,** 429–449.

Gal-Chen, T., and R. C. J. Somerville 1975 On the use of coordinate transformations for the solution of the Navier-Stokes equations. *Mon. Wea. Rev.*, **17,** 207–228.

Haltiner, G. J., and R. T. Williams 1980 *Numerical Prediction and Dynamic Meteorology, 2nd Ed.* John Wiley, New York. 477pp.

Janjić, Z. I. 1989 On the pressure gradient force error in $\sigma$-coordinate spectral models. *Mon. Wea. Rev.*, **117,** 2285–2292.

Johnson, D. R., T. H. Zapotocny, F. M. Reames, B. J. Wolf, and R. B. Pierce 1993 A comparison of simulated precipitation by hybrid isentropic-sigma and sigma models. *Mon. Wea. Rev.*, **121,** 2088–2114.

Kasahara, A. 1974 Various vertical coordinate systems used for numerical weather prediction. *Mon. Wea. Rev.*, **102,** 509–522.

Konor, C. S., and A. Arakawa 1997 Design of an atmospheric model based on a generalized vertical coordinate. *Mon. Wea. Rev.*, **125,** 1649–1673.

Laprise, R. 1992 The Euler equations of motion with hydrostatic pressure as an independent variable. *Mon. Wea. Rev.*, **120,** 197–207.

Mesinger, F., and Z. I. Janjić 1985 Problems and numerical methods of the incorporation of mountains in atmospheric models. *Lectures in Applied Mathematics*, **22,** Part 2, 81–120. B. Engquist, S. Osher and R. C. J. Somerville (editors), American Mathematical Society, Providence, RI.

Phillips, N. A. 1957 A coordinate system having some special advantages for numerical forecasting. *J. Meteor.*, **14,** 184–185.

Simmons, A. J., and D. M. Burridge 1981 An energy and angular momentum conserving vertical finite-difference scheme and hybrid vertical coordinates. *Mon. Wea. Rev.*, **109,** 758–766.

Simmons, A. J., and R. Strüfing 1981 An energy and angular momentum conserving finite-difference scheme, hybrid coordinates and medium-range weather prediction. ECMWF Technical Report No. 28, 68 pp.

Uccellini, L. W., D. R. Johnson, and R. E. Schlesinger 1979 An isentropic and sigma coordinate hybrid numerical model: Model development and some initial tests. *J. Atmos. Sci.* **36,** 390–414.

Zhu, Z., J. Thuburn, B. J. Hoskins, and P. H. Haynes 1992 A vertical finite-difference scheme based on a hybrid $\sigma$-$\theta$-$p$ coordinate. *Mon. Wea. Rev.*, **120,** 851–862.

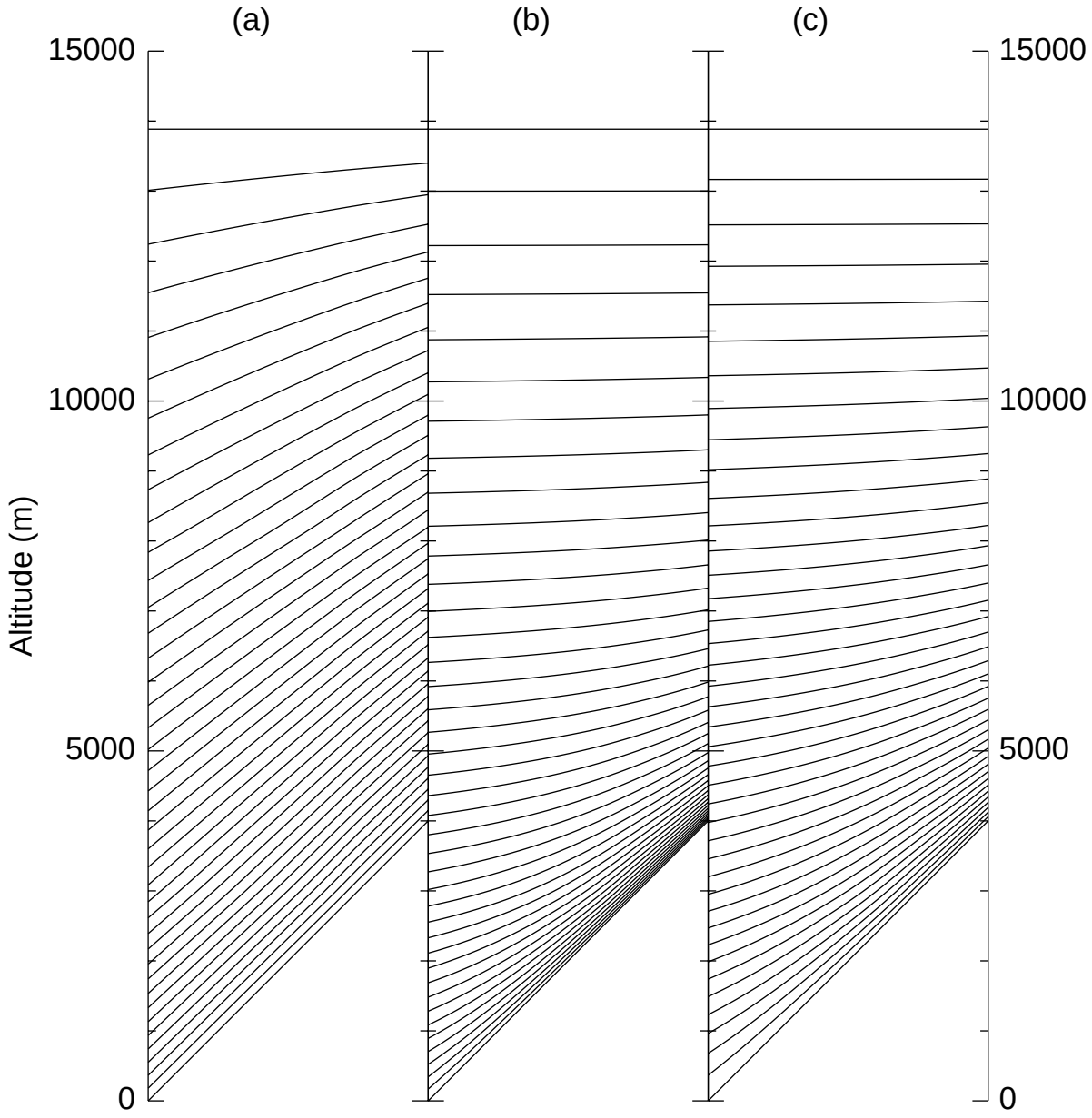


Figure 1. (a) The disposition of modified sigma coordinates, $\hat{\sigma}$, at uniform spacing assuming a model top at $p_t = 180$ mb with terrain sloping to 4 km. (b) Pressure-sigma hybrid coordinates defined by (2.7) for $p_L = 1100$ mb and with $\tau = 0.2$. (c) Same as (b) but with $\tau = 0.5$.

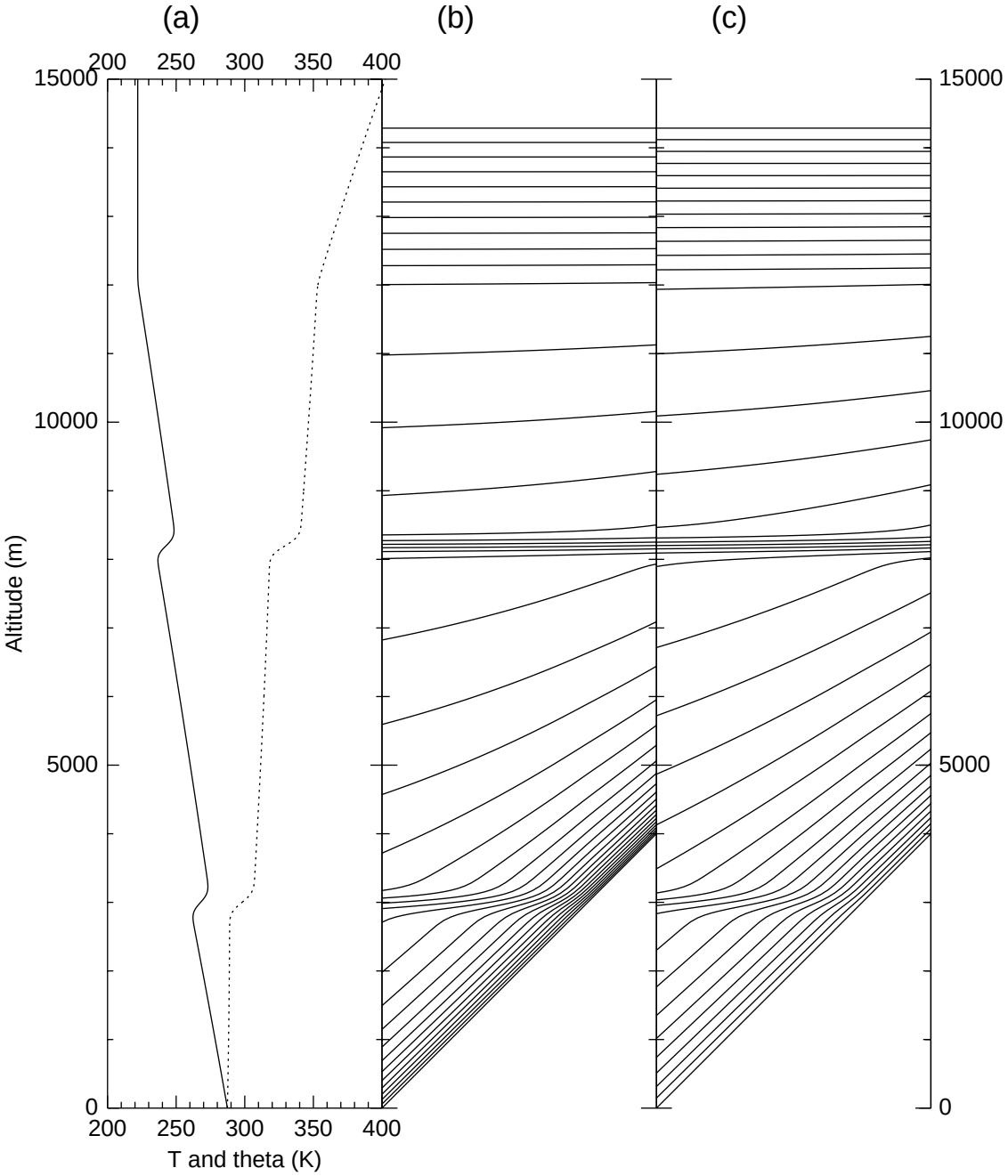


Figure 2. (a) A vertical profile of temperature (solid) and corresponding potential temperature (dotted) for a stratified synthetic atmosphere with an approximately isentropic layer up to an inversion at around 3 km and a tropopause at around 12 km. (b) The uniformly spaced theta-sigma hybrid coordinates for this stratification and with the parameters defined in (2.12)–(2.14) and $\tau = 0.2$. (c) Same as (b) but with $\tau = 0.5$

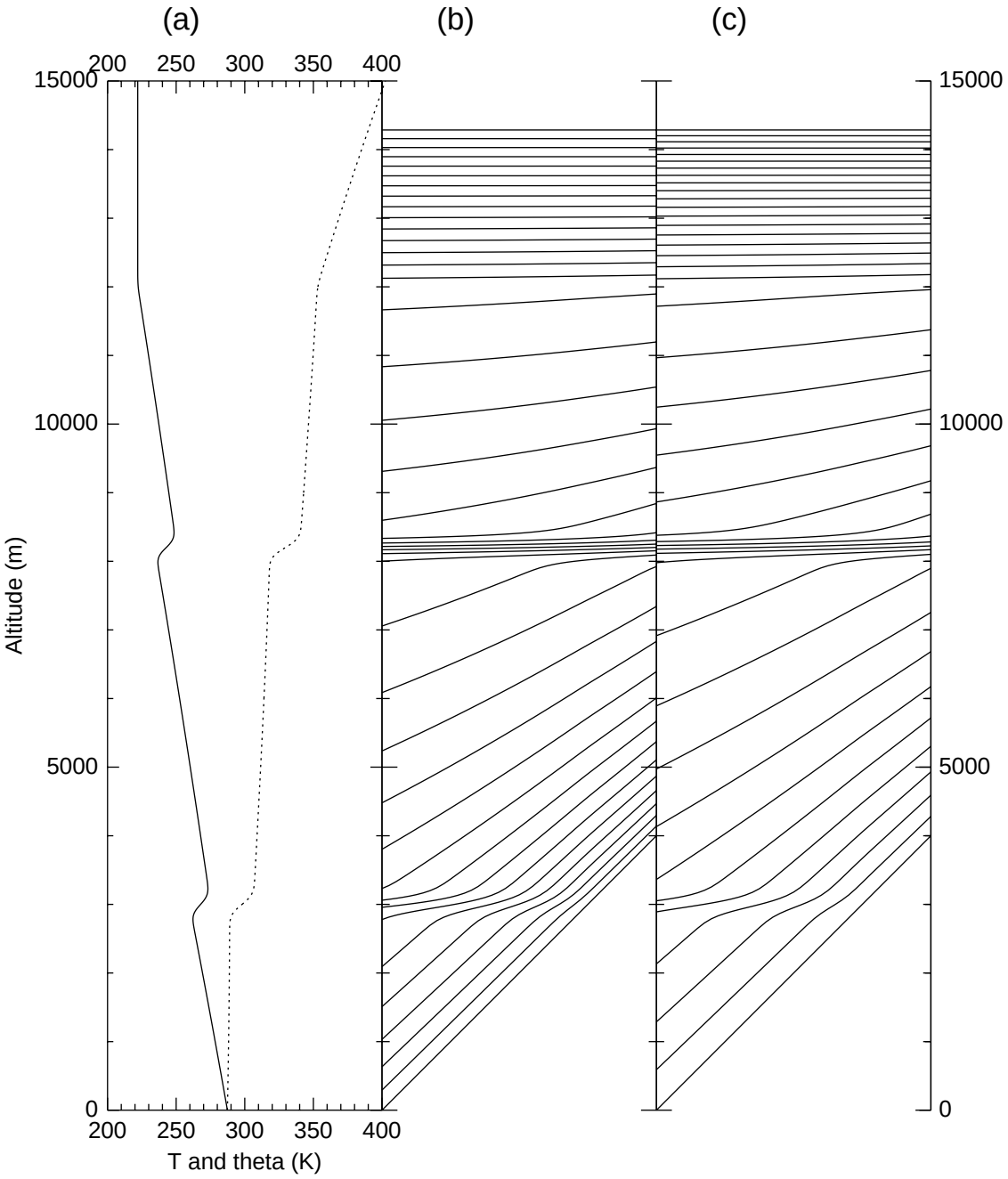


Figure 3. Same as Fig. 2 but with: (b) $\tau = 1.0$; (c) $\tau = 2.0$.

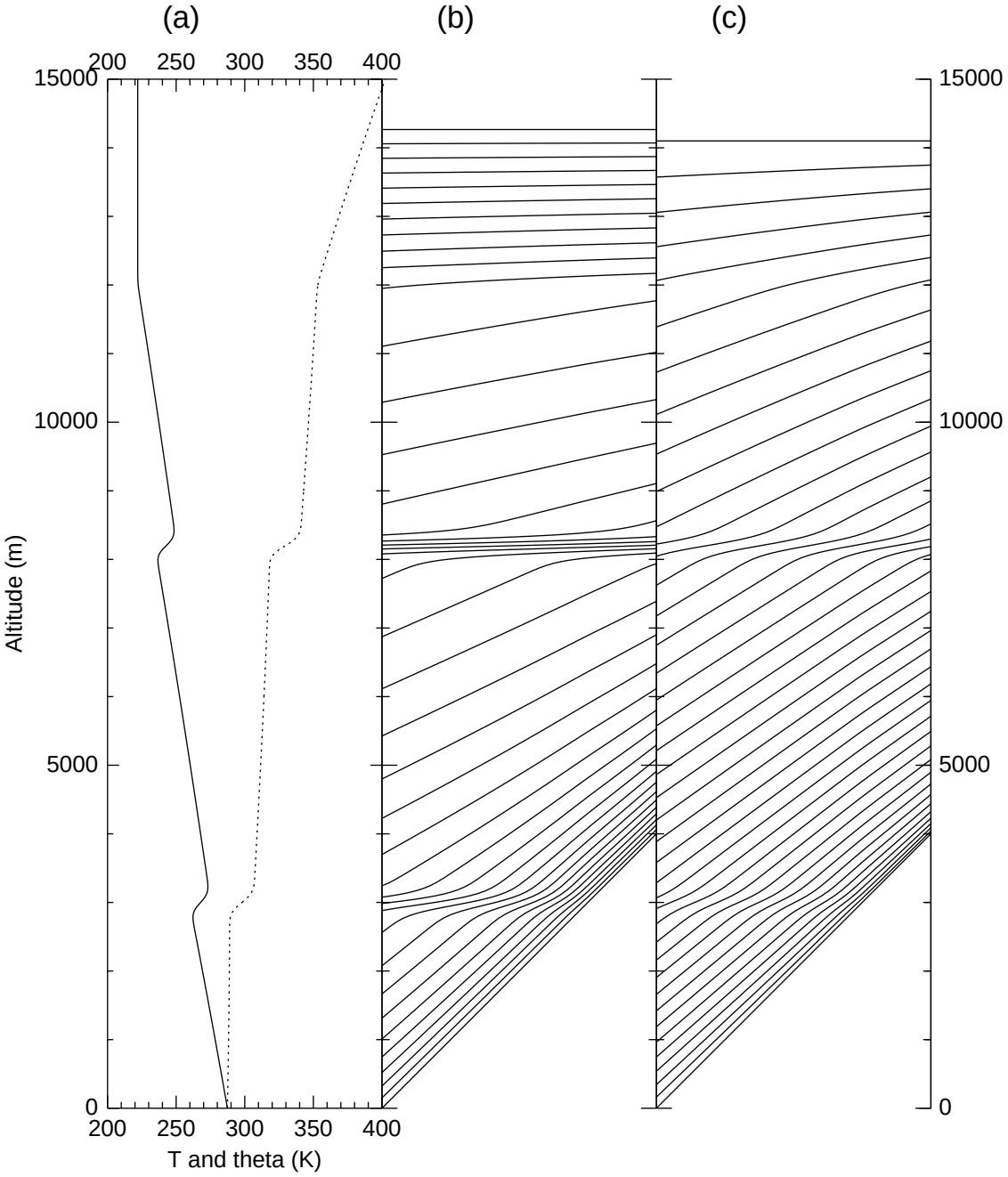


Figure 4. Same as Fig. 2(c) with $\tau = 0.5$, but with: (b) $\alpha = 0.2$; (c) $\alpha = 0.8$

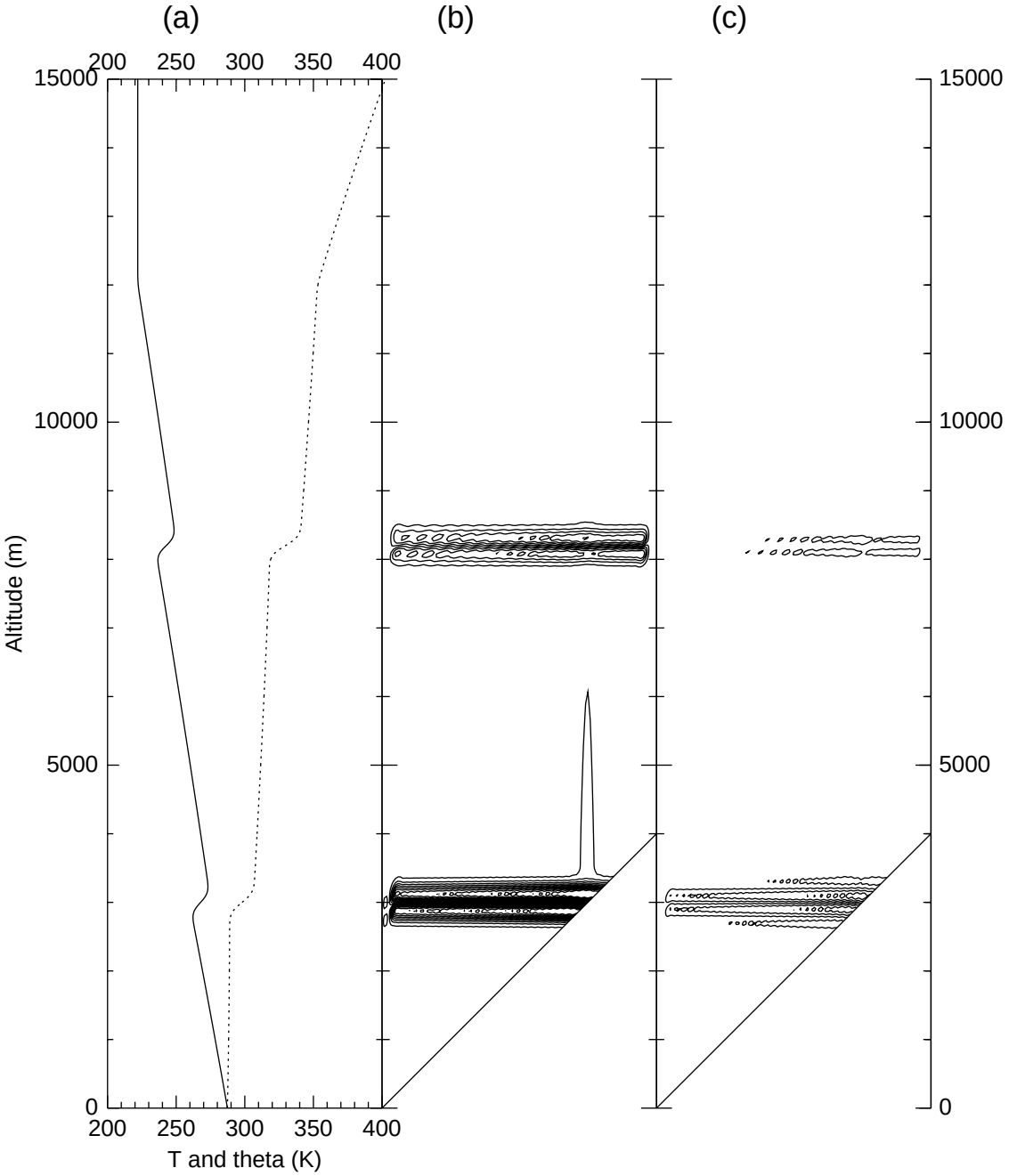


Figure 5. The same profile (a) as in previous figures, together with contours of the numerical error incurred in evaluating the horizontal pressure gradient force using derivatives of pressure and geopotential. The vertical coordinates are the sigma coordinates. No numerical error is assumed for operations in the vertical direction. In the horizontal, we assume the grid of 40 spaces spans the domain of width 600 km (i.e., a 15 km grid spacing. The error contours, being in units of $10^{-5}$m s$^{-2}$, translate to units of $10^{-1}$m s$^{-1}$ in equivalent geostrophic wind when a value of $10^{-4}$s$^{-1}$ is taken for a typical midlatitude Coriolis parameter. (b) the errors using second-order horizontal differencing; (c) using conventional centered fourth-order differencing.

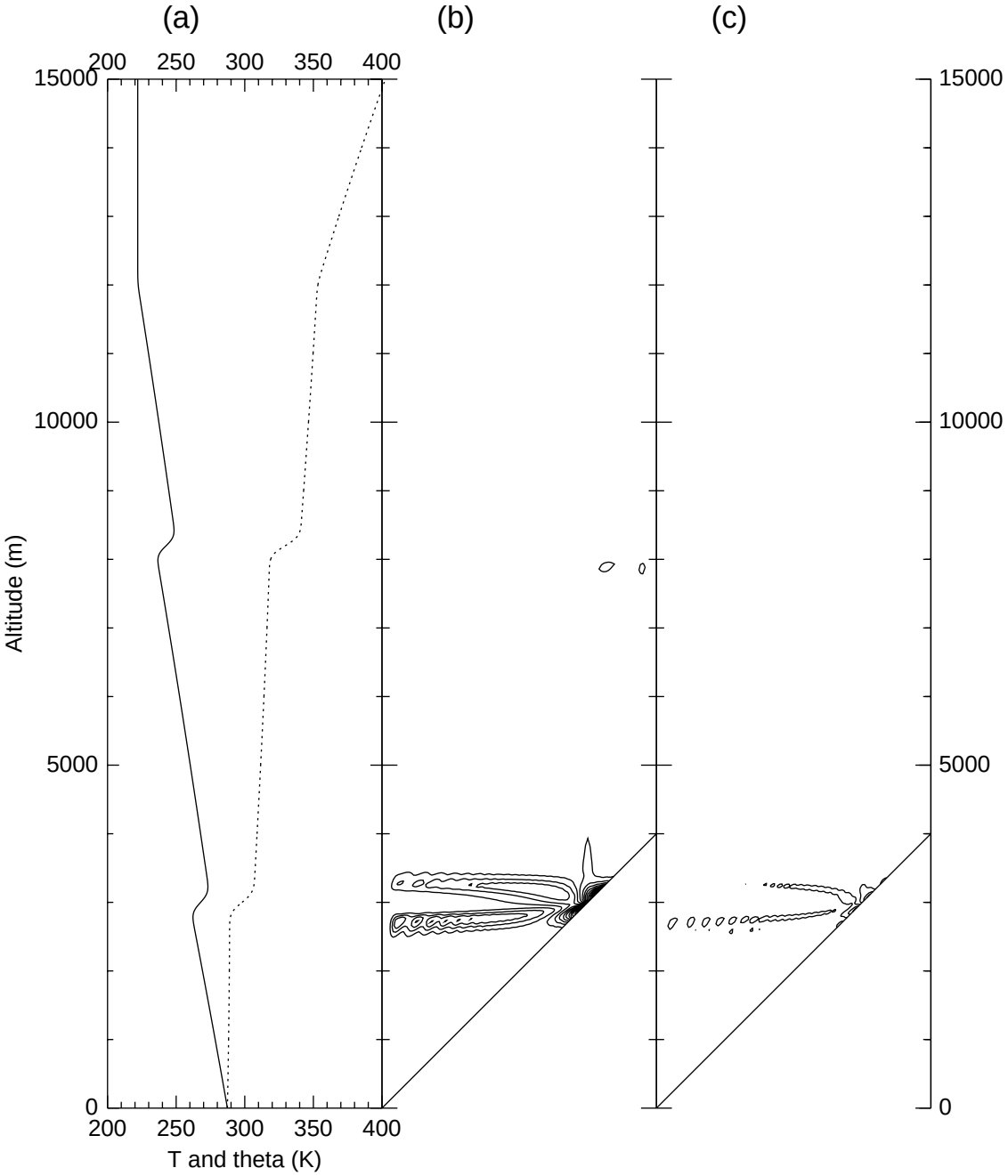


Figure 6. Same as Fig. 5 but using the hybrid coordinates of Fig. 2(c) with $\tau = 0.5$.

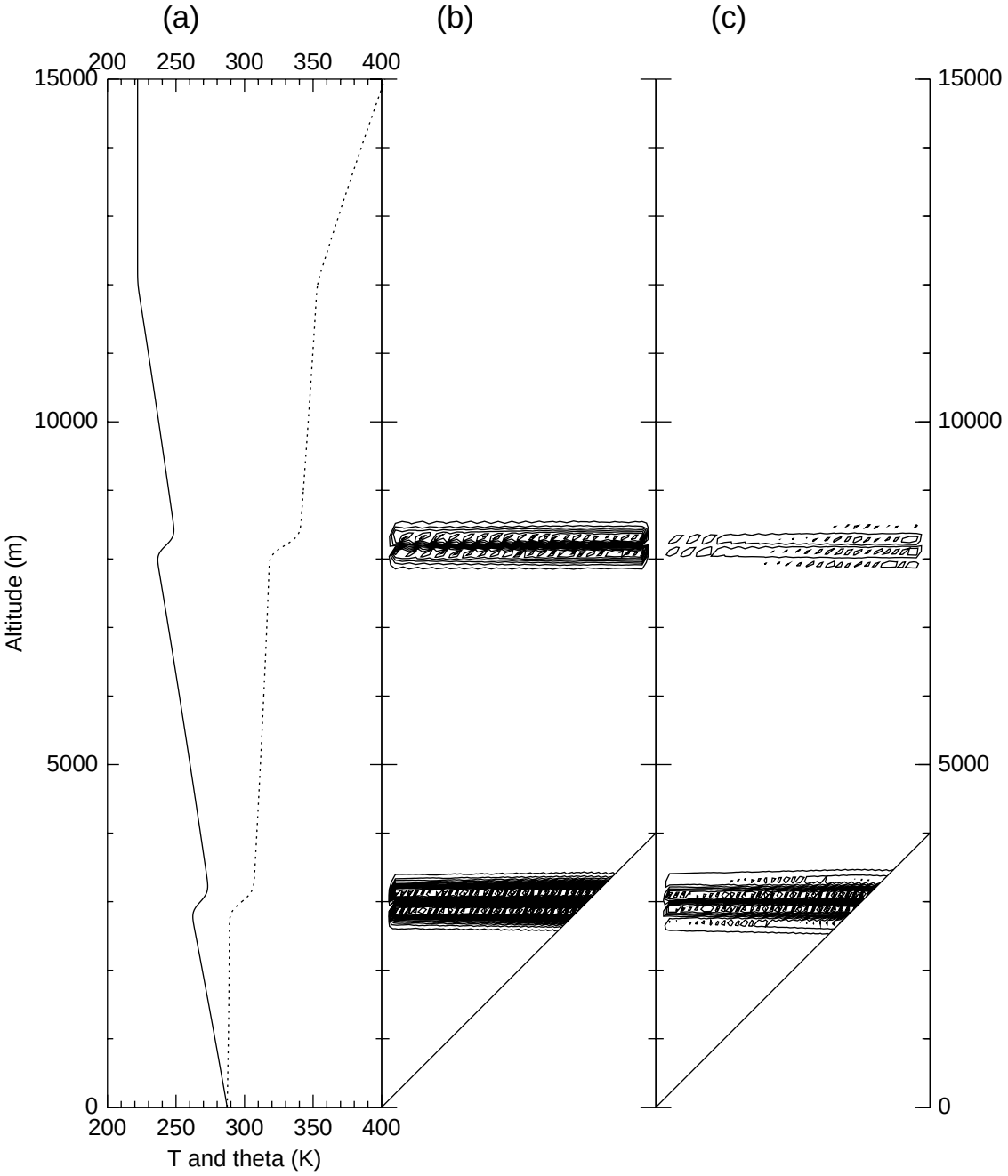


Figure 7. Same as Fig. 5 but estimating the horizontal pressure gradient force using the derivatives of the Montgomery potential and potential temperature on the sigma coordinates.

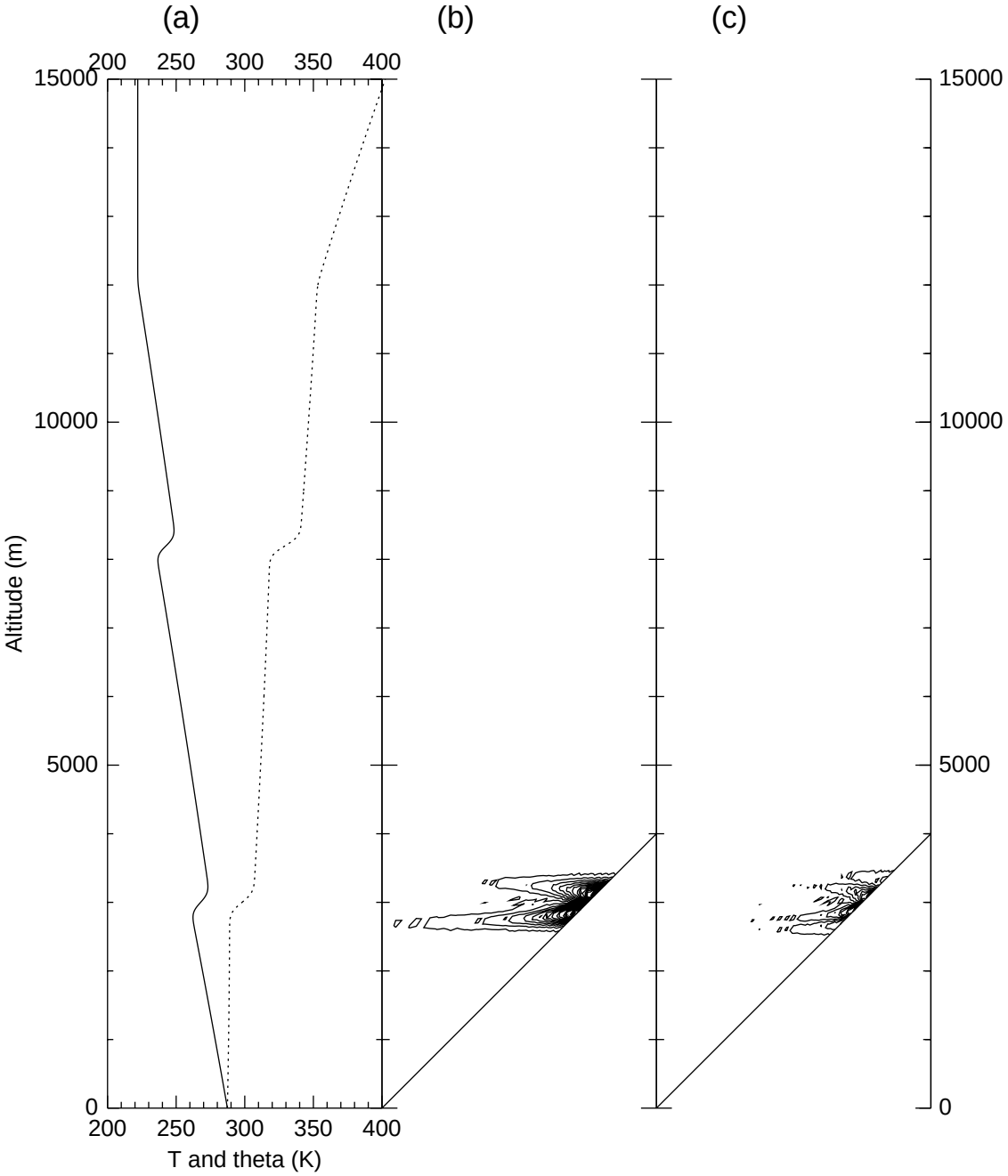


Figure 8. Same as Fig. 7 but using the hybrid coordinates of Figs. 2(c) and 6 with $\tau = 0.5$

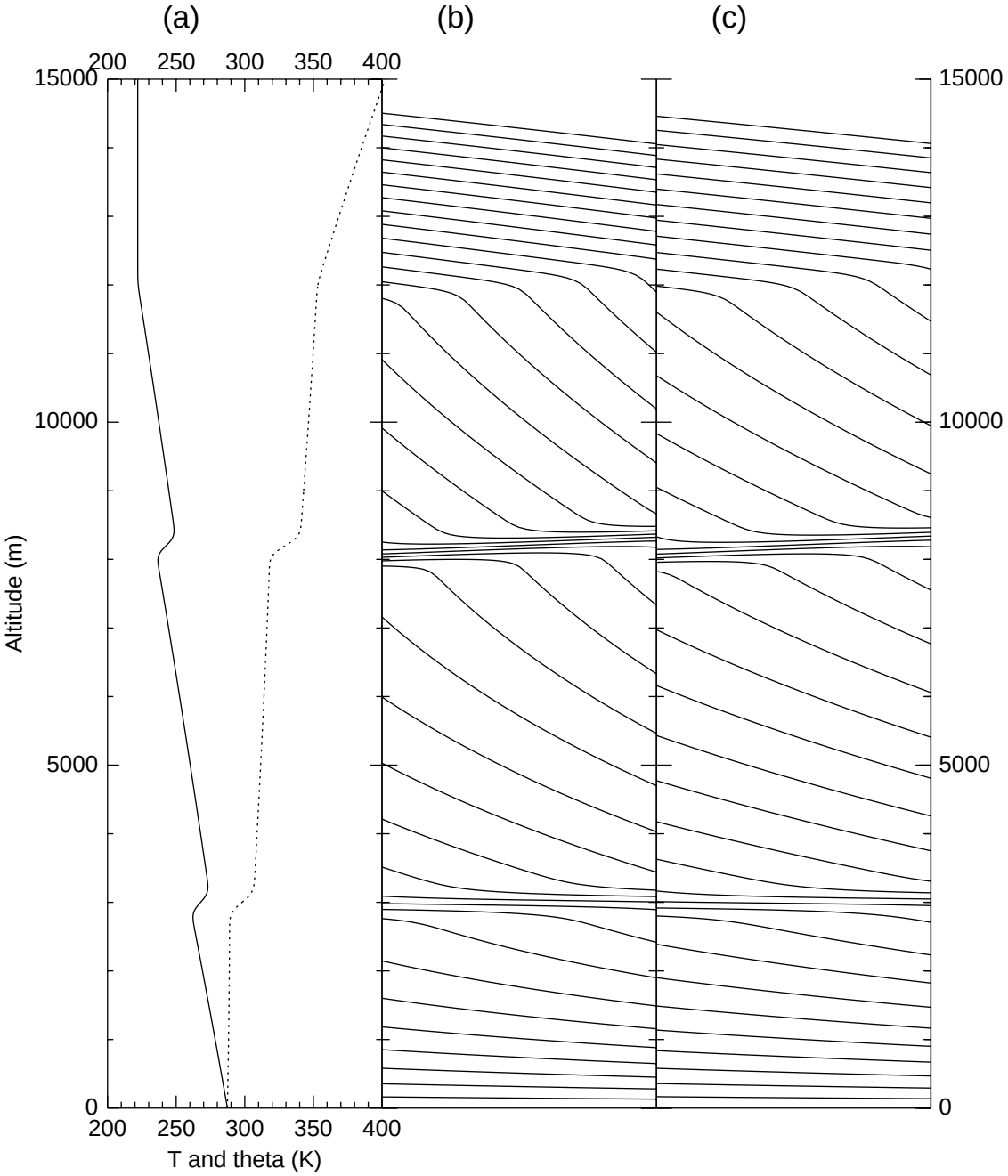


Figure 9. (a) The previously used thermal profile that now applies to the center of the domain, in which a horizontal thermal gradient along constant pressure surfaces of 0.25K per grid unit (still 15km) is imposed. In this case, there is no orography and the surface pressure is kept constant. (b) The hybrid coordinates with previously defined constants except $\tau = 0.5$ and $\alpha = 0.$. (c) Same as (b) except $\alpha = 0.2$

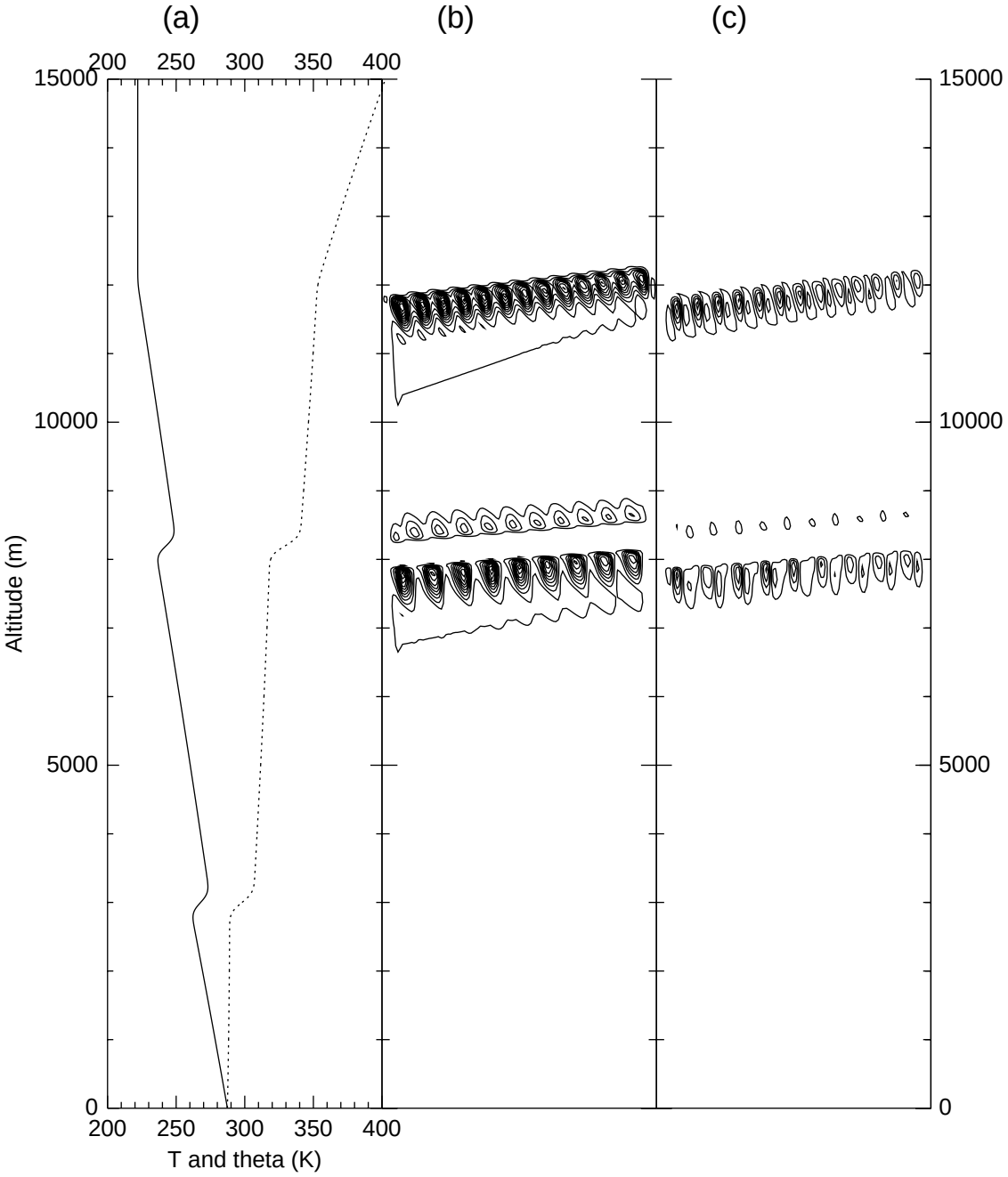


Figure 10. (a) Central domain thermal profile as in Fig. 9. (b) Errors in the horizontal pressure gradient in the hybrid coordinates of Fig. 9(b) when using derivatives of pressure and geopotential with second-order derivatives. (c) Same as (b), but using fourth-order derivatives.

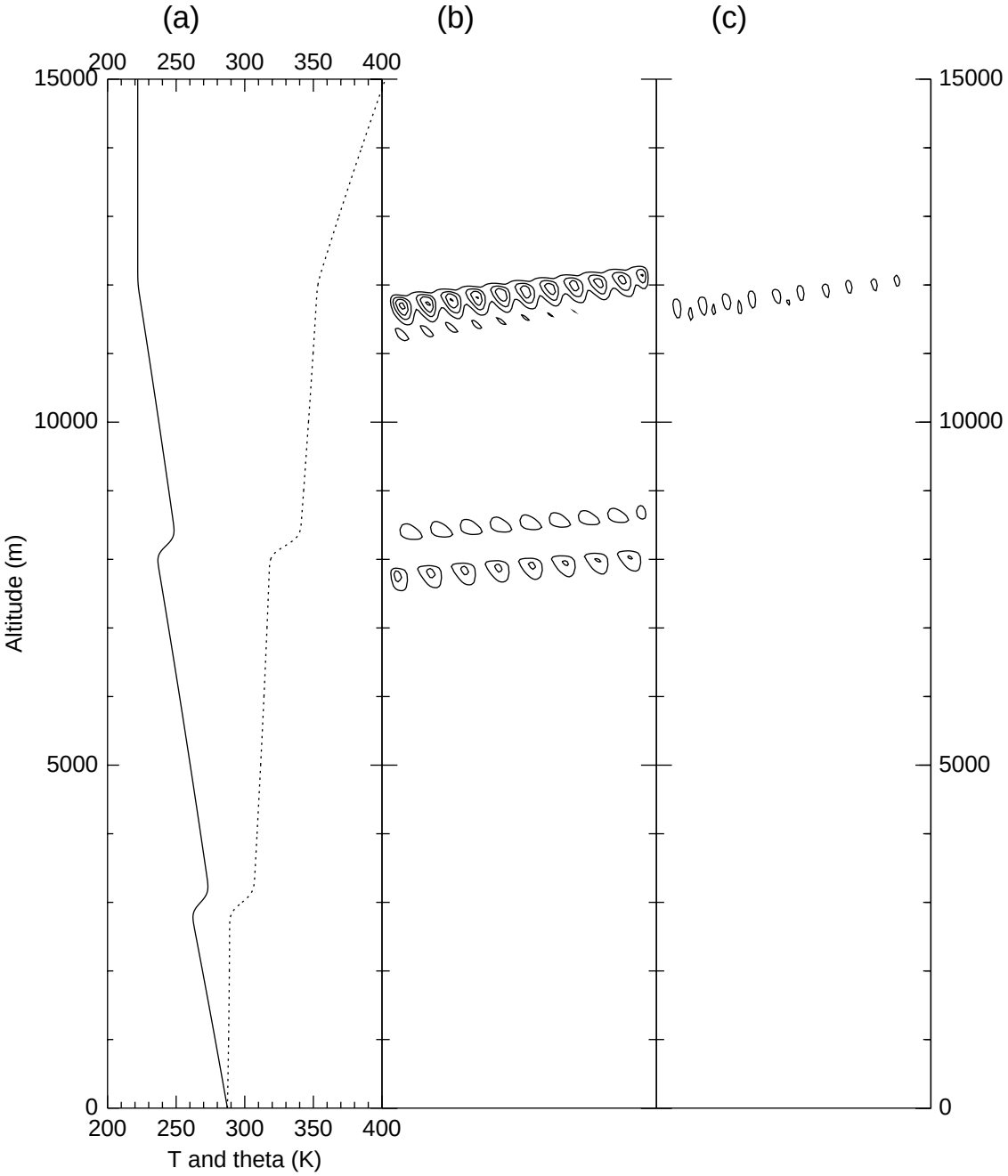


Figure 11. Same as Fig. 10, but for the hybrid coordinates of Fig. 9(c) in which $\alpha = 0.2$